Egypt. J. Chem. **Vol. 67,** No. 6 pp. 95 - 104 (2024)

Egyptian Journal of Chemistry

http://ejchem.journals.ekb.eg/

Cost-effective biosorption of ammonium ion from aqueous solutions using *Corchorus olitorius L.* leaves

Ahmed A.I. Abd-Ellatif [1,2], Mohamed N. Rasheda [1], Mohamed A.M. Raslan [1,3], Salah G.A. Ali [4], Gomaa A. M. Ali [5,6,*]

[1] *Department of Chemistry, Faculty of Science, Aswan University, 81528, Aswan, Egypt*

[2] *Sohag Drinking water & Sanitation Company, 82515, Sohag, Egypt*

[3] *Faculty of Technological Industry and Energy, Thebes Technological University, 85863, Thebes, Luxor, Egypt*

[4] *Department of Botany and Microbiology, Faculty of Science, Al-Azhar University, 71524, Assiut, Egypt*

[5] *Chemistry Department, Faculty of Science, Al-Azhar University, Assiut 71524, Egypt*

[6] *Faculty of Science, Galala University, 43511, Suez, Egypt*

Abstract

To remove ammonium ions at a low cost, this study utilized Corchorus olitorius leaves biosorbents. Various removal parameters are conducted to find the best ammonium removal method. They are the initial ammonium concentration, the adsorbent dose, the contact time, and pH. The fitted equilibrium data were accurately described and analyzed using the Freundlich, Temkin, Langmuir, and Dubinin-Radushkevich models. Langmuir isotherm model R^2 (0.9982), which has a maximum saturated monolayer sorption capacity of 5.62 mg g^{-1}, was particularly amenable to the developed method. Good agreement was found between the experimental value of qe (4.05 mg g^{-1}) and calculated values of qe (4.14 mg g^{-1}), demonstrating that the adsorption process follows pseudo-second-order kinetics and resulting in a high value of R^2 (0.9993). The adsorption procedure was conducted at various temperatures to assess how temperature impacts the thermodynamic parameters. Consistently negative values for ΔG_o across a wide temperature range demonstrate the spontaneity of biosorption reactions. Exothermicity (ΔH_o = -91.98 kJ mol^{-1}) was measured during adsorption. A lower value for $\Delta S°$ at the solid solution interface between ammonium and adsorbent denotes less disorder and randomness in the system. The results of the experiments show that the leaves of the inexpensive and widely available plant Corchorus olitorius have a remarkable effect on ammonium ions removal from aqueous solutions.

Keywords: Bioadsorption, C. olitorius L. leaves, Ammonium ion, Water treatment, Environment.

1. Introduction

Ground water contains many undesirable metals, including ammonia, that affect potable water quality. Ammonia can exist as either the ammonium ion (NH_4^+) or as ammonia (NH_3), depending solely on the pH. The prevailing pH levels in most soils and groundwater indicate that ammonium is the predominant form. Nevertheless, these two species are often used interchangeably, referred to generally as "ammonia". Ammonium ion NH_4^+ was the direct reason for neglecting many wells because of the exceeding of their concentrations of the values set out in the Minister of Health's decision in 2007 (0.5 mg L^{-1}). The detection of ammonia in a drinking water source typically suggests that a nearby source containing ammonia is in close proximity to the water intake [1]. The anthropogenic sources responsible for ammonia contamination near water intakes are typically associated with waste products derived from animals or humans. Ammonia, even in low concentrations (0.2 mg L^{-1}), poses a toxic threat to fish and various aquatic organisms [2].

Recently, significant research effort has been focused on investigating the elimination of unwanted materials from drinking water through the process of adsorption, utilizing agricultural materials [3-8]. Adsorption is one of the most effective treatment strategies as it does not require high temperatures and can simultaneously adsorb many chemicals [9-15].

Water treatment technology plays a pivotal role in advancing and achieving sustainable development goals, particularly in ensuring the availability and sustainable management of water and sanitation. Water treatment technologies help ensure the provision of safe and clean drinking water to communities, thereby contributing to Goal 6 (Clean Water and Sanitation) by increasing access to potable water sources. Water treatment technology is a critical tool for addressing multiple aspects of sustainable development, with a direct impact on Goal 6 but also significant contributions to several other interconnected goals. It serves as a cornerstone for fostering environmental sustainability, economic growth, public health, and social well-being.

Corchorus olitorius L. (C. olitorius L.), known as Jew mallow or jute mallow (English) and Molokheiya (Arabic), is a plant species that belongs to the Tiliaceae family. The cost of growing jute mallow is meager, and it can grow on roadsides [16, 17], in fields, and in-home gardens [18]. It is widely consumed as a vegetable in most parts of Africa [19]. In Egypt, the cultivation of *C. olitorius L.* encompassed approximately 12,583.8 acres of land. Each harvest yielded an average total production of 2.5-3 tons, and the crop was

*Corresponding author e-mail: gomaa-sanad@azhar.edu.eg

eceive Date: 19 September 2023, Revise Date: 25 October 2023, Accept Date: 27 November 2023

DOI: 10.21608/EJCHEM.2023.237655.8641

typically harvested four times throughout the cultivation season. The plant was cultivated year-round in Egypt, with outdoor cultivation during summer and indoor cultivation in greenhouses [20]. Many adsorbents as banana peel, orange peel [21], pomegranate peel [22], and watermelon rind [23] are not good options for large-scale use due to collections of large quantities suitable to use in water treatment plants are not quickly processed, and may need high cost to collection and storage, also a large quantity of it not commercially available. However, otherwise dry *C. olitorius L.* leaves can be collected in large quantity to use in water treatment plants, as it commercially available by large quantity with low cost, easily available, environmentally friendly and does not create secondary pollution and can be stored for a long time [24]. It is possible to exploit the significant areas in the drinking water stations in Egypt to grow the mallow plant and use it to remove ammonia from the groundwater, especially since most of the stations have fertile agricultural soil. The present study demonstrates the adsorption efficiency of *C. olitorius L.* leaves.

2. Materials and Methods

2.1 Characterization techniques

The X-ray diffractometer (XRD, PW1710, Philips, Cu-Kα radiation with λ= 1.542 Å) was utilized to study the materials crystal structure. The measurement was conducted with a step of 0.023 from 4° to 70°. Fourier transform infrared (FTIR, range from 400 to 4000 cm^{-1}) spectroscopy was performed using an ATR-FT-IR spectrometer from Bruker. High-resolution scanning electron microscopy (SEM) was carried out using the Quanta FEG 250 SEM with a field emission gun from FEI Company, Netherlands. In addition, Elemental analysis was performed using a Thermofisher pathfinder instrument under low vacuum conditions, operating at an accelerating voltage of 20–30 kV, and employing a large field detector with a working distance of 15–17 mm. The N_2 adsorption-desorption technique with BELSORP max II equipment from Japan was utilized to measure the samples' specific surface area, pore size and pore volume. Prior to analysis, the sample underwent overnight outgassing at 70 ºC under a vacuum of 0.00001 Torr. The BET equation was applied to calculate the BET surface areas, while the Barrett-Joyner-Halenda (BJH) method was used to estimate the pore size distributions (PSD). To measure the residual ammonia concentration in the supernatant, a spectrophotometer model DR6000 from Germany was employed. The pH adjustments were made using a pH meter model Orion-4-star from Thermo Scientific, USA. Stirring of the adsorption mixture at 300 rpm was achieved using a magnetic stirrer model F20500011 from Velp Scientifica-Italy. Distilled water was produced using a fully Automatic Single Water Still model A4000 from Stuart Aquatron.

2.2 Treatment of Corchorus olitorius L.

The leaves of *C. olitorius L.* used as an adsorbent in this study were obtained from agriculture, rinsed multiple times with tap water, and then distilled. Subsequently, it was dried naturally in the sun, broken into small fragments, and ground to achieve more petite dimensions.

2.3 Stock ammonia solution

Anhydrous NH_4Cl (3.819 g) dried at 100 °C was dissolved in distilled water to make the stock ammonia solution. The solution was then diluted to a final volume of 1000 mL. In this solution, 1.00 mL is equivalent to 1.00 mg of nitrogen (N) or 1.22 mg of ammonia (NH_3), following the method outlined in 4500 NH_3-F [25].

2.4 Procedure

The batch adsorption system was six 100 ml beakers in each 25 mL ammonia solution and 0.1g of *C. olitorius L.* leaves (4 g L^{-1}). Then the system was adequately shaken by a magnetic stirrer to appreciate contact time at 300 rpm. After that, filtration through the filter paper and the remaining ammonia concentration in wastewater was determined according to method 4500 NH_3-F [25].

3. Results and Discussion

3.1 Characterization of the biosorbent

3.1.1 BET analysis

Fig. 1 presents N_2 adsorption-desorption isotherm of *C. olitorius L.* leaves. The corresponding pore diameter, pore volume, and surface area were measured to be 3.5222 nm, and 0.071225 $cm^3\ g^{-1}$, and 12.672 $m^2\ g^{-1}$, respectively. The results indicate that *C. olitorius L.* leaves have a significantly greater surface area, while the pore volumes are relatively similar. Compared to other low-cost biosorbents such as sorghum plant waste, wheat straw, corn straw, bagasse sugarcane (SCB), orange peels (OPS), Arundo donax L. treated with NaOH, Napier grass, and Olive stone. *C. olitorius L.* leaves have a large surface area (Table 1). Pore volume describes the saturation of the pore with N_2 at the most significant relative pressure (P/P_o), where P/P_o = 0.99. It is expected that C. olitorius L should adsorb more cations, given its larger surface area.

Table 1: Surface area comparison of *C. olitorius L.* leaves with other biosorbents.

Biosorbent	**S_{BET} ($m^2\ g^{-1}$)**	**[Ref.]**
Sorghum	0.9	[26]
Modified sorghum	0.14	[26]
Wheat straw	12.576	[27]
Corn straw	10.235	[27]
Bagasse Sugarcane (SCB)	4.90	[28]
Orange peels (OPS)	1.24	[28]
Arundo donax L. treated with NaOH	2.86	[29]
Napier grass	4.05	[30]
Olive stone	0.38	[31]
C. olitorius L. leaves	12.672	This study

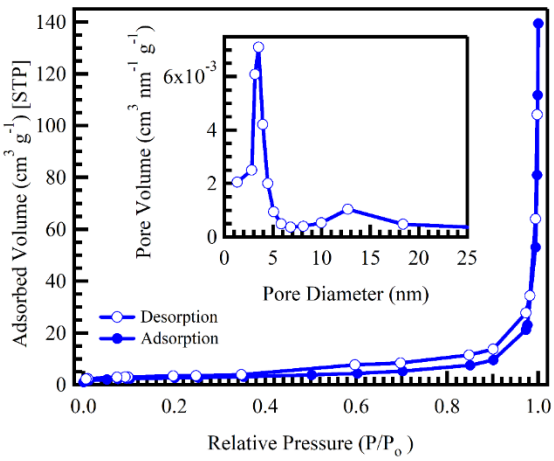

Fig. 1. N_2 adsorption-desorption isotherm of *C. olitorius L. leaves; the inset is the pore size distribution.*

3.1.2 X-ray diffraction

Fig. 2 displays that after ammonium ion adsorption, the *d-spacing* of all characteristic peaks in the used sample increases from 5.92, 4.02, 3.52, 2.36, 1.95, and 1.72 nm in the fresh sample to 6.10, 4.04, 3.53, 2.38, 1.96, and 1.73 nm in the used sample, respectively, indicating adsorption of at least a layer of ammonium ion on the surface of *C. olitorius L.* leaves biosorbent.

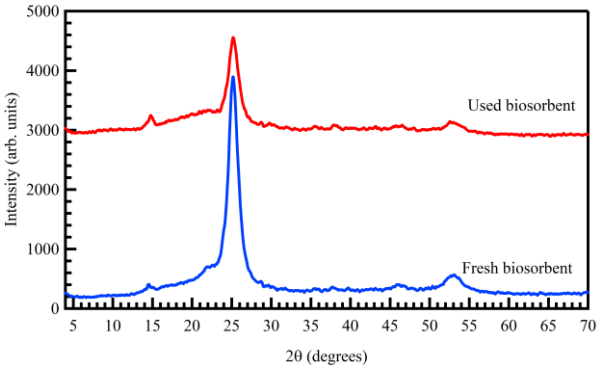

Fig. 2. XRD patterns of *C. olitorius L.* leaves: fresh and used biosorbents.

3.1.3 Infrared spectroscopy

Fig. 3 shows the difference between the FT-IR spectra of *C. olitorius L.* leaves taken before and after the biosorption of ammonium ions. It shows how the vibration frequencies of functional groups change. Regarding FT-IR analysis after ammonium ion uptake, modifications to carbonyl C=O and phenolic -OH groups were evident. The absorption peaks of *v* (-C-O-), *v* (-C=O-), *v* (-C=C), and *v* (-OH) in *C. olitorius L.* changed from 1049.82 to 1032.44, 1648.15 to 1544.88 to 3348.74 cm^{-1}, before and after ammonium ion sorption, respectively. The presence of C=O, phenolic -OH groups on the biosorbent surface, and the chemical interaction between the adsorbate and these groups, all suggest that these groups play a role in the biosorption process.

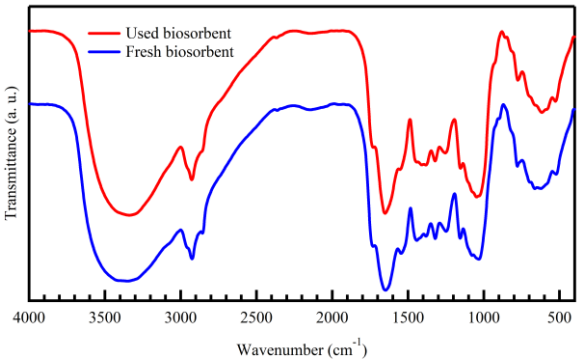

Fig. 3. FTIR analyses of *C. olitorius L.* leaves: fresh and used biosorbents.

3.1.3 SEM photographs

Before the adsorption of ammonium ions, SEM images (Fig. 4) of the *C. olitorius L.* leaves revealed asymmetric pores that were rough and cylinder-shaped. Their rough surface enhances these asymmetric pores' interaction with ammonium ions. In addition, the SEM image shows that after ammonium ion adsorption, the surface of *C. olitorius L.* leaves is smooth and shiny with closed pore structures. This is likely due to a physicochemical interaction between functional groups on the *C. olitorius L.* leaves surface and the ammonium ions.

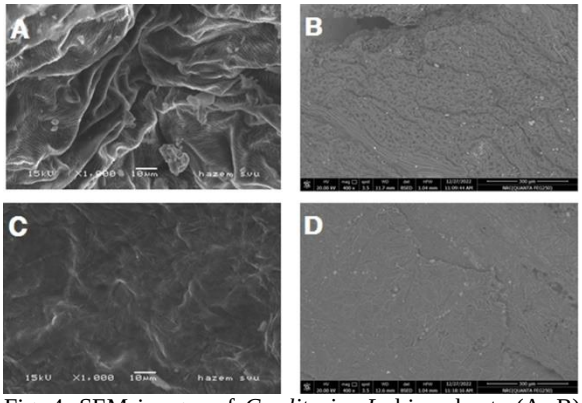

Fig. 4. SEM images of *C. olitorius L.* biosorbents (A, B) fresh, (A at magnification power 1000- B at magnification power 400) and (C, D) used biosorbents (C at magnification power 1000- D at magnification power 400).

3.1.4 Energy dispersive X-ray analysis

The SEM-EDX technique was conducted on random samples to verify the presence of the various components in *C. olitorius L.* leaves. This scanning was performed over a large area. *C. olitorius L.* biosorbent elemental concentrations were analyzed. SEM-EDX analysis confirmed that only peaks for the targeted elements were present in the *C. olitorius L.* biosorbent. The concentration of different elements on the granular surfaces of the *C. olitorius L.* biosorbent was determined by taking readings from a series of cross-sectional marks. The percentage of atomic nitrogen in a fresh sample (before adsorption) increased to 17.03%, as shown in Fig. 5. This suggests that the leaves of *C. olitorius L.* are absorbing ammonium ions.

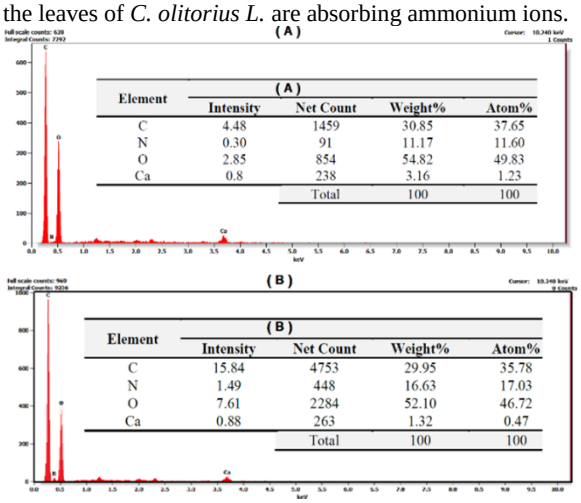
(A)

Element	Intensity	Net Count	Weight%	Atom%
C	4.48	1459	30.85	37.65
N	0.30	91	11.17	11.60
O	2.85	854	54.82	49.83
Ca	0.8	238	3.16	1.23
		Total	100	100

(B)

Element	Intensity	Net Count	Weight%	Atom%
C	15.84	4753	29.95	35.78
N	1.49	448	16.63	17.03
O	7.61	2284	52.10	46.72
Ca	0.88	263	1.32	0.47
		Total	100	100

Fig. 5. EDX of *C. olitorius L.* leaves: fresh (A) and used (B) biosorbents.

3.2 The influence of different factors on ammonium ion adsorption by C. olitorius L.

3.2.1 pH effect

The effects of pH on adsorption are dramatic. The ionization of functional groups on the sorbent surface is affected by the pH of the surrounding solution, which is in part due to the competitive influence of H^+ ions [32]. At room temperature, the influence of pH on ammonium adsorption was investigated by changing the pH value from 3 to 8. pH 6 with 81.0% removal was optimal, as shown in Fig. 6a. As the pH of the solution dropped, so did the removal percentage. More

H^+ in acidic solutions means more effective competition with NH_4^+ cations, leading to a lower removal percentage. At pH levels above 6, ammonium ions are converted to NH_3 gas, resulting in a lower removal percentage [33, 34]. Emmerson et al. [33] found that NH_4^+ ions convert to NH_3 gas at pH above 7, whereas at pH below 7, ammonium primarily exists as NH_4^+.

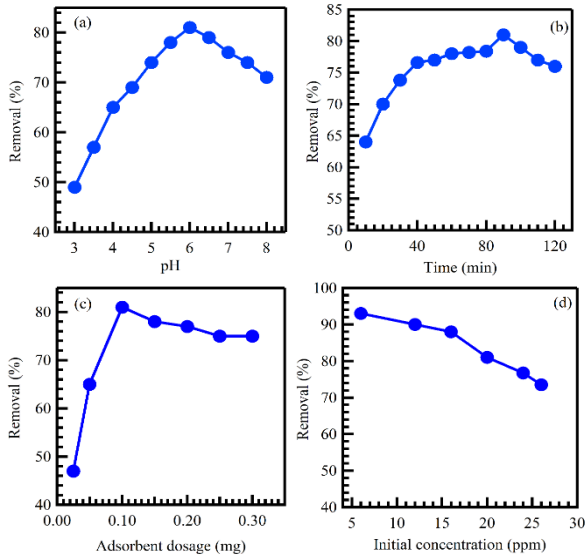

Fig. 6. Influence of pH (a), contact time (b), dosage (c), and initial concentration (d) on NH_4^+ adsorption on *C. olitorius L.* leaves.

3.2.2 Influence of contact time

As can be seen in Fig. 6b, the percentage of waste removed steadily increased over the course of 90 minutes. Adsorption was initially shown to remove the target substance quickly and effectively. This is because of the high concentration of active sites, primarily carboxylic (-COO) and hydroxyl (-OH) groups, available due to the large surface area. These active sites were crucial in improving the adsorption efficiency and, consequently, the removal rates as a whole [35]. The rate at which NH_4^+ is removed from a solution decrease with increasing contact time between the sorbent material and the solution. The removal rate drops dramatically after 90 minutes, indicating that no more NH_4^+ are being removed from the solution. With the system in equilibrium, the removal rate drops because fewer active sites on the sorbent are available.

3.3.3 Influence of adsorbent dose

By changing the amount of C. olitorius L. used from 25.0 to 300 mg while keeping all other variables the same, the effect of the adsorbent dose was examined as shown in **F**ig. 6c. The removal rate of NH_4^+ increases dramatically with an increase in the C. olitorius L. dose [36, 37] due to an increase in adsorbent surface area and the availability of more adsorption sites. When the dose was more significant than 0.1 g, the highest removal percentage (81.0%) occurred at 0.1 g. Aggregation of adsorption sites reduced the total adsorbent surface area, reducing the removal percentage.

3.3.4 Influence of initial ammonium concentration

At room temperature, the influence of initial concentration on the adsorption rate was studied by using a range of NH_4^+ concentrations (6.0, 12, 16, 20, 24, and 26 mg L^{-1}), as shown in Fig. 6d. It was observed that the efficiency of ammonium removal decreased as the initial concentration of ammonium increased. This outcome happens because *C. olitorius's* active sites become full once the ammonium ion concentration gets high enough. Similar findings were made for ammonia removal by the pomegranate peel powder [22].

3.3 Adsorption isotherm

The behavior of adsorbates in contact with adsorbents can be described using isotherms. There is a wide variety of adsorption isotherms. Temkin, Frendulich, Langmuir, and D-K isotherms were used in this investigation.

3.3.1 Langmuir isotherm

The Langmuir isotherm theory presumes that the adsorption energy is constant, and that no transmigration of adsorbate molecules is observed if adsorbate molecules are assumed to form a monolayer over a homogeneous adsorbent surface where all sorption sites are identical. To describe the Langmuir adsorption isotherm, the following equation is used [38].

$$q_e = \frac{q_m K_L C_e}{1 + K_L C_e} \qquad (1)$$

where K_L (L mg^{-1}) is the Langmuir isotherm constant and q_m (mg g^{-1}) is the maximum adsorption capacity. The Langmuir relation can be linearized in the most common form as follows [38]:

$$\frac{C_e}{q_e} = \frac{1}{K_L q_m} + \frac{1}{q_m} C_e \qquad (2)$$

Ammonium ion adsorption onto *C. olitorius L.* leaves at 25 ℃ is shown as a linear fit in Fig. 7a, using the Langmuir isotherm model. Measurements of q_m, K_L, and R^2 are listed in Table 2: Since R^2 was 0.9982, it was clear that the adsorption data would be well-fit by the Langmuir equation [39], a very high coefficient of determination. Ammonium ions were adsorbed onto the surface of *C. olitorius L.*, creating a monolayer. The surface is homogeneous. Upon adsorption of ammonia onto pomegranate peel powder, it adhered in a monolayer, aligning with the predictions of the Langmuir model [22]. The Langmuir isotherm can be characterized by the separation factor R_L, which is a dimensionless constant. The R_L factor provides a measure of the adsorption process's favorability [40, 41] as shown by the following equation:

$$R_L = \frac{1}{1 + K_L C_0} \qquad (3)$$

where C_0 (mg L^{-1}) is the highest $[NH^+_4)]^0$. In Table 2, the R_L values, ranging from 0.04 to 0.18, were found to be less than unity. R_L represents the shape of the isotherm and can be classified as linear (R_L = 1), unfavorable (R_L > 1), favorable (0 < R_L < 1), or irreversible (R_L = 0). The R_L values observed indicate that the adsorption of ammonium onto *C. olitorius L.* is a favorable process. Therefore, *C. olitorius L.* demonstrates itself as a promising adsorbent for ammonium ions.

Table 2. Separation factor at an initial concentration of ammonium ion.

C_0 (mg L^{-1})	R_L
6	0.1750
12	0.0960
16	0.0738
20	0.0599
24	0.0501
26	0.0467

3.3.2 Freundlich isotherm

Adsorption on a heterogeneous surface with molecule-molecule interactions is assumed by the Freundlich exponential equation. Adsorbate concentration is assumed to increase (Fig. 7b) and so is the adsorbate concentration on the adsorbent surface, according to this model [42].

The Freundlich constant (KF), which characterizes the adsorption capacity, and 1/nF, which signifies the adsorption intensity, serve as indicators not only of the energy distribution but also of the heterogeneity of the adsorbent sites. These parameters offer valuable insights into both the relative distribution of energy and the variation in adsorption sites within the adsorbent material [43]. The linear forms of Freundlich are given as [38]:

$$\ln q_e = \ln K_F + \frac{1}{n_F}\ln C_e \qquad (4)$$

Table 3 shows that Freundlich has a lower R^2 value (0.9479) than Langmuir (0.9982). Therefore, unlike the Freundlich model, the Langmuir model is more applicable to the adsorption of ammonium ions on *C. olitorius L.* with a value of 0.427 for 1/n, the adsorption process is favorable but no heterogeneity has been observed (the adsorption is favorable when $0.1 < 1/n < 1$).

3.3.3 Temkin isotherms

The Temkin model is applicable for assessing the adsorption capacity of an adsorbent towards a specific adsorbate. According to this model, the heat of adsorption for molecules within an adsorption layer increases as the thickness of the adsorbate layer on the adsorbent surface increases. This increase in heat of adsorption is linearly reduced with the increasing coverage of the adsorbate layer [44]. The linear form of Temkin model is represented by Eq. (5) as follows [11]:

$$Q_e = \frac{RT}{2.303B_T}\log K_T + \frac{RT}{2.303B_T}\log C_e \qquad (5)$$

In the given context, B_T is the Tempkin constant associated with the heat of sorption (in J mol^{-1}), T denotes the absolute temperature of the solution (K), R represents the gas constant (8.314 J mol^{-1} K^{-1}), and K_T is the Tempkin isotherm constant (in L g^{-1}). The relationship between Q_e and log C_e, as plotted in Fig. 7c, demonstrates a linear correlation. The values determined for BT and KT are 0.387 KJ mol^{-1} and 8.01 L g^{-1}, respectively.

3.3.4 Dubinin–Radushkevich Isotherm

Typically, this model was used to separate the effects of chemical and physical adsorption on metal ions by calculating their respective mean free energies [45]. Physisorption is assumed to be occurring when the adsorption energy (E_D) is less than 8.0 kJ mol^{-1} (Fig. 7d). However, chemisorption will occur if the E_D is between 8 and 16 kJ mol^{-1} [46]. Surfaces can be homogeneous or heterogeneous, and the Dubinin-Radushkevich model works for both [47]. The linear form of the Dubinin-Radushkevich model is:

$\ln q_e = \ln s - k_D\varepsilon^2$ (6)

In the given context, the DR monolayer capacity constant is denoted as qs (mg g^{-1}), the DR constant associated with adsorption energy is represented by KD (Mol^2 $K^{-1}J^{-2}$), and the Polanyi's potential, which relates to the free energy of adsorption, is indicated by ε (KJ^2 Mol^{-2}). The Polanyi's potential ε is given from the following formula:

$$\varepsilon = RT\ln\left(1+\frac{1}{C_e}\right) \qquad (7)$$

and the E_D can be calculated from:

$$E_D = \frac{1}{\sqrt{2K_D}} \qquad (8)$$

Table 3 displays the results of the calculation for E_D; the value is 1.97 KJ mol^{-1}. This means that adsorption of one mole of ammonium ion from an infinitely dilute solution onto the surface of *C. olitorius L.* requires a free energy change of 1.97 KJ mol^{-1}. When E_D is less than 8 KJ mol^{-1}, physisorption occurs. In addition, Table 4 compares of ammonium adsorption capacities using some related adsorbents.

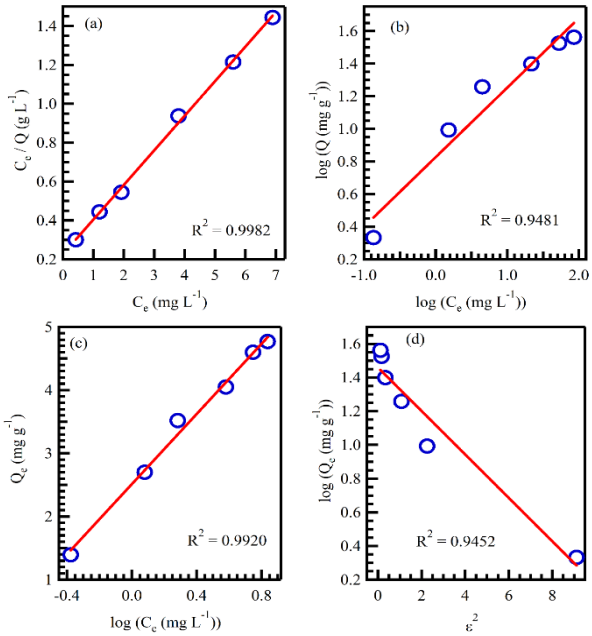

Fig. 7. Sorption isotherm for ammonium ion adsorption on *C. olitorius L.* leaves, Langmuir (a), Freundlich (b), Tempkin (c), and Dubinin–Radushkevich (d).

Table 3: Langmuir, Freundlich, Temkin, and Dubinin-Radushkevich constants for the adsorption of ammonia onto *C. olitorius L.* leaves (T = 298 K, time= 90 min, Initial concentration of ammonia = 20 mg L^{-1}, pH = 6, volume of solution = 0.025 L, DL dosage = 0.1 g).

Langmuir			
Q_m (mg g^{-1})	K_L (L mg^{-1})	R^2	
5.62	0.784	0.9982	
Freundlich			
$1/n_F$	K_F (L mg^{-1})	R^2	
0.427	2.29	0.9479	
Temkin			
K_T (KJ mol^{-1})	B_T	R^2	
8.01	0.387	0.992	
Dubinin-Radushkevich			
Q_s (mg g^{-1})	K_D (mol^2 $K^{-1}J^{-2}$)	E_D (KJ mol^{-1})	R^2
4.3	0.1289	1.97	0.9452

Table 4: Comparison of ammonium adsorption capacities using some related adsorbents.

Adsorbate	Characteristics	Removal of Ammoniom ions		Ref.
Volcanic tuff	50.02 m^2 g^{-1}	19.00 mg g^{-1}	60-70%	[32]
Strawberry leaves Strawberry stems Boston ivy leaves Boston ivy stems Southern magnolia leaves Poplar leaves	0.35 m^2 g^{-1} 0.10 m^2 g^{-1} 31.96 m^2 g^{-1} 0.53 m^2 g^{-1} 1.54 m^2 g^{-1}	6.71 mg g^{-1} 4.62 mg g^{-1} 6.07 mg g^{-1} 5.01 mg g^{-1} 6.22 mg g^{-1} 6.25 mg g^{-1}	37.65% 37.93% 52.71% 38.12% 44.37% 42.00%	[48]
Pomegranate peel powder	Particle size 10-750 µm	6.18 mg g^{-1}	88%	[49]
Biochar obtained from rice straw	Attractive material contains silica with amorphous ash contant The total pores 1.3 cm^3 g^{-1}	4.251 mg g^{-1}	43%	[50]
Modification bentonite	90.894 m^2 g^{-1}	5.85 mg g^{-1}	75%	[51]
Light expanded clay aggregate	A special type of clay pelletized (with grains size 4–10 mm)	0.255 mg g^{-1}	----	[52]
Coconut shell-activated carbon	Specific surface area 198 m^2 g^{-1}	2.48 mg g^{-1}	58-93%	[53]
Posidonia oceanic fibres	Fiber with 0.1 mm diameter and 20–30 mm length	1.73 mg g^{-1}	----	[54]
Bentonite	Particle size of 0.00-0.05 mm	4.92 mg g^{-1}	55.7%	[55]
H_2O_2-modified zeolitic waste	138.89 m^2 g^{-1}	0.23 mg g^{-1}	72%	[56]
Biochar from exhausted coffee husk	60.982 m^2 g^{-1}	1.13 mg g^{-1}	----	[57]
C. olitorius L. leaves	12.672 m^2 g^{-1} Asymmetric pores, rough and cylinder-shaped	5.62 mg g^{-1}	*81.0%*	This work

3.4 Adsorption kinetic models

Researchers have used various kinetic models to learn more about the adsorption process, model the adsorption procedure, and predict the physisorption and chemisorption processes [58]. Specifically, the pseudo-first-order [59], the pseudo-second-order [60], and the Elovich model [61] were used to conduct the analysis.

3.4.1 Pseudo-first-order equation

Lagergren's relation [62] provides the following pseudo-first-order model:

$$q_t = q_e\left(1 - e^{-K_1 t}\right) \qquad (9)$$

where k_1 is the rate constant of adsorption (min^{-1}), q_t represents the amount adsorbed at time t (min), and q_e represents the amount of ammonium ion adsorbed (mg g^{-1}) at equilibrium.

The linearized form of the PFO model is as follows.

$$\ln(q_e - q_t) = \ln q_e - K_1 t \qquad (10)$$

Based on the slope and intercept of the ln(qe-qt) vs. t plots, the values of k_1 and q_e were determined. The results in Fig. 8a and Table 5 confirm the low R^2 values and the poor agreement between the experimental and calculated qe values. This demonstrates that the kinetics of ammonium adsorption onto *C. olitorius L.* leaves do not follow the first order.

3.4.2 Pseudo-second-order equation

Ho et al. [63] provided the pseudo-second-order equation as follows:

$$\frac{t}{q_t} = \frac{1}{K_2 q_e^2} + \frac{1}{q_e} t \qquad (11)$$

where k_2 (g mg^{-1} min^{-1}) is the pseudo-second-order adsorption rate constant.

Fig. 8b shows a plot of t/q_t vs. *t*, from which we can determine the values of q_e and k_2. Excellent agreement was found between the experimental and calculated qe values, and Table 5 shows that R^2 values are very high. Because of this, pseudo-second-order kinetics adequately describes the adsorption of ammonium onto *C. olitorius*. Adsorption data for ammonium onto *C. olitorius L.* can be described in terms of a second-order kinetics equation, suggesting that the adsorption process is likely chemisorption and that the rate-determining step. Adsorption isotherms for ammonium ions onto pomegranate peels showed comparable patterns [22].

Table 5. PFO and PSO models for the adsorption of ammonium onto *C. olitorius L.* leaves.

Pseudo First Order	$[NH_4)]^0$ (mg L^{-1})	q_e, exp (mg g^{-1})	q_e, cal (mg g^{-1})	k_1 (min^{-1})
	20	4.05	0.874	0.027
Pseudo Second Order	q_e, cal (mg g^{-1})	k^2 (g mg^{-1} min^{-1})	R^2	
	4.14	0.069	0.9993	
Elovich	t_0 min	a (g mg^{-1} min^{-1})	1/b (mg g^{-1})	R^2
	0.00115	311.87	0.3584	0.9648

3.4.3 Elovich model

Chemical adsorption kinetics can be modeled using the Elovich equation [61]. In many cases, the Elovich equation holds true for systems with a heterogeneous adsorbing surface [64]. Elovich's equation has been used to successfully describe the adsorption of pollutants from aqueous solutions in recent years [65, 66]. Here is Elovich's equation:

$$q_t = \frac{1}{b}\ln(t + t^0) - \frac{1}{b}\ln(t^0) \qquad (12)$$

where $t^0 = 1/ab$, If $t >> t^0$, the equation can be simplified to the linearized form as follows:

$$q_t = \frac{1}{b}\ln(t) + \frac{1}{b}\ln(ab) \qquad (13)$$

In the context of this study, 'a' represents the initial adsorption rate (mg g^{-1} min^{-1}), while the parameter 1/b (mg g^{-1}) is related to the availability of adsorption sites.

Plotting q_t against ln(t) results in a linear relationship, as depicted in Fig. 8c. From the intercept and slope of the line, the values of a = 311.87 (mg g^{-1} min^{-1}) and 1/b = 0.3584 (mg g^{-1}) were obtained. These parameters, along with the rest of the parameters, are summarized in Table 5. Among all the models considered, the pseudo-second-order model proves to be the most appropriate for accurately representing the experimental data.

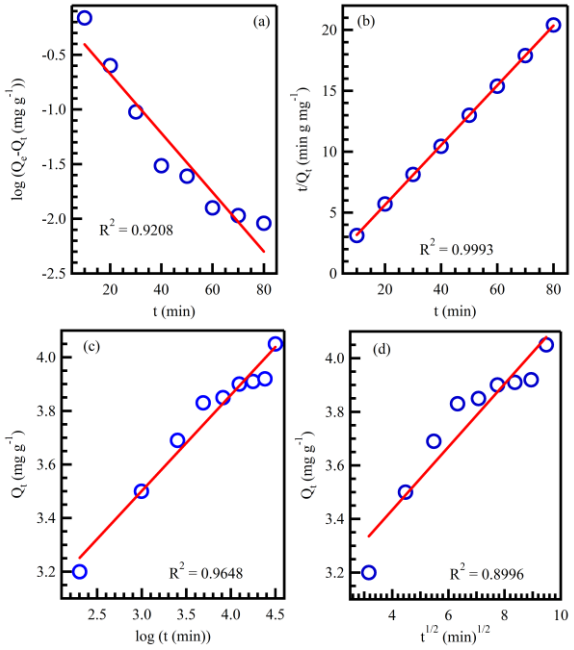

Fig. 8. Kinetic curves: pseudo-first-order (a), pseudo-second-order (b), simple Elovich (c), and intraparticle diffusion (d) models for ammonium ions adsorption on *C. olitorius L.* leaves.

3.4.4 Intraparticle diffusion model

The intraparticle diffusion of solute in adsorbents is interpreted using the Weber-Morris model [67]. This is an expression of the Weber-Morris model [68]:

$$q_t = K_p t^{\frac{1}{2}} + C \qquad (15)$$

Where k_p is the intraparticle diffusion rate constant (mg g^{-1} $min^{-1/2}$)), calculated from the slope, and C (mg g^{-1}) is the intercept of the plot of q_t vs. $t^{0.5}$, which represents the thickness of the boundary layer [69]. When a straight line passes through the origin of a plot (Fig. 8d), it indicates that sorption is primarily influenced by pore diffusion. This suggests that solute ions diffuse within the pores and capillaries of the adsorbent material [70]. However, as seen in Fig. 8d, if the plot loses its linearity, the film diffusion process is assumed to be the rate-limiting step.

3.5 Adsorption thermodynamics

Thermodynamic parameters, such as the entropy change (ΔS°), enthalpy change (ΔH^0), and free energy change (ΔG^0), can shed light on the adsorption process. These values can be used to learn more about the adsorption process and its characteristics. The Van't Hoff equation, which describes the correlation between temperature and the equilibrium constant, is written as follows [71]:

$$\Delta G° = \Delta H° - T\,\Delta S° \qquad (16)$$

$$\ln K^{o} = -\frac{\Delta H^{o}}{RT} + \frac{\Delta S^{o}}{R} \qquad (17)$$

Where T is the absolute temperature in Kelvin (K), R is J K^{-1} mol^{-1}, and Ke° is the thermodynamic equilibrium constant. To find the entropy change (ΔS°), plot ln(Ke°) against 1/T and take the intercept. The plot's slope can also determine the enthalpy change (ΔH°). To determine the thermodynamic equilibrium constant (Ke°), Lima et al. use the following equation [72].

$$K_L^{o} = \frac{1000.kL.\text{molecular weight of adsorbate}).[\text{Adsorbate}]^{o}}{\gamma} \qquad (18)$$

In the given context, γ represents the coefficient of activity (dimensionless), and [Adsorbate]° denotes the standard concentration of the adsorbate (mol L^{-1}). It is assumed that the adsorbate solution is sufficiently diluted, allowing us to consider the activity coefficient as unity.

Table 6 displays all the thermodynamic parameters. Since *Δ*H° is negative, ammonia adsorption on *C. olitorius L.* must be exothermic. Reduced disorder and randomness at the ammonia-adsorbent solid solution interface are represented by a negative value of *Δ*S°. Adsorption is spontaneous and preferential when *Δ*G° is negative. Xu et al. [73] and Cheng et al. [51] reported identical outcomes. Adsorption is physisorption if the enthalpy change is less than 20 kJ mol^{-1} [74]. For this system, the *Δ*H° values were less than 20 kJ mol^{-1}, indicating physisorption adsorption.

The cost-effective biosorption of ammonium ions using C. olitorius L. leaves has the potential to offer sustainable and practical solutions for addressing water pollution, agricultural nutrient management, and environmental remediation, with positive implications for water quality, ecosystem health, and sustainable resource management.

Table 6. Calculated thermodynamic parameters for ammonia adsorption on C. olitorius.

T (K)	K_L L mg^{-1}	K_L^0	Ln K_L^0	ΔG° (kJ mol^{-1})	ΔH° (kJ mol^{-1})	ΔS° (J mol^{-1} K^{-1})
298	0.784	14137.17	9.5566	-23.47	-91.7	-228.96
308	0.1878	3388.26	8.13	-21.18		
313	0.1145	2065.88	7.633	-20.04		
318	0.0795	1433.74	7.268	-18.89		

4. Conclusion

In this work, the potential of C. olitorius L. leaves for removing ammonium ions from aqueous solutions was explored as an efficient, safe, and cost-effective natural material that can be cultivated in roadside areas and home gardens. The adsorption of ammonium ions onto *C. olitorius L.* leaves was confirmed through XRD, SEM, and EDX analyses, while FT-IR analysis highlighted the significant roles played by hydroxyl and carboxyl groups in the adsorption process. The optimal adsorption conditions were identified as follows: pH 6.0, an absorbent dosage of 4 g L^{-1}, a contact time of 90 minutes at 298 K. Equilibrium isotherm data fitting revealed a good agreement with the Langmuir model, showing a maximum saturated monolayer sorption capacity of 5.62 mg per gram (5.62 mg g^{-1}). Kinetic

studies in this research indicated that the data conformed well to the pseudo-second-order model (R^2 = 0.9993). The sorption process was found to be exothermic, as evidenced by the negative entropy value (-ΔS), signifying a decrease in the freedom of the adsorbed species. Furthermore, the Gibbs' free energy (ΔG°) exhibited a negative value, suggesting that the adsorption occurs spontaneously. The findings underscore the highly effective nature of *C. olitorius L.* leaf biomass as a sorbent for the removal of ammonium ions from wastewater.

References

[1] Sadegh H., Ali G.A.M., Abbasi Z., Nadagoud M.N. Adsorption of Ammonium Ions onto Multi-Walled Carbon Nanotubes. Studia Universitatis Babes-Bolyai Chemia, 62(2), 233-245 (2017).

[2] Haralambous A., Maliou E., Malamis M., The use of zeolite for ammonium uptake, Water Sci. Technol., 1992, pp. 139-145.

[3] Habeeb O.A., Ramesh K., Ali G.A.M., Yunus R.M. Experimental design technique on removal of hydrogen sulfide using CaO-eggshells dispersed onto palm kernel shell activated carbon: Experiment, optimization, equilibrium and kinetic studies. Journal of Wuhan University of Technology-Mater. Sci. Ed., 32(2), 305-320 (2017).

[4] Habeeb O.A., Ramesh K., Ali G.A.M., Yunus R.M. Low-cost and eco-friendly activated carbon from modified palm kernel shell for hydrogen sulfide removal from wastewater: adsorption and kinetic studies. Desalination and Water Treatment, 84, 205-214 (2017).

[5] Adam M.R., Othman M.H.D., Hubadillah S.K., Abd Aziz M.H., Jamalludin M.R. Application of natural zeolite clinoptilolite for the removal of ammonia in wastewater. Materials Today: Proceedings, https://doi.org/10.1016/j.matpr.2022.12.207 (2023).

[6] Pathan A., Prajapati C.G., Dave R.P., Bhasin C.P. Effective and Feasible Photocatalytic Degradation of Janus Green B dye in Aqueous Media using PbS/CTAB Nanocomposites. International Journal of Thin Film Science and Technology, 11(2), 245-255 (2022).

[7] Mampilly R.B., Bhatt S.H., Modi N.J., Pathan A. Adsorption of Eriochrome Black-T dye by batch investigations using waste tea@Fe NPs as low-cost adsorbent. International Journal of Thin Film Science and Technology, 13(1), 17-25 (2024).

[8] Mampilly R.B., Pathan A., Bhasin C.P. Visible Light-Assisted Degradation of Malachite Green dye using Waste Tea-Mediated Zinc Nanoparticles. International Journal of Thin Film Science and Technology, 12(1), 39-51 (2023).

[9] Maazinejad B., Mohammadnia O., Ali G.A.M., Makhlouf A.S.H., Nadagouda M.N., Sillanpää M., Asiri A.M., Agarwal S., Gupta V.K., Sadegh H. Taguchi L9 (34) orthogonal array study based on methylene blue removal by single-walled carbon nanotubes-amine: Adsorption optimization using the experimental design method, kinetics, equilibrium and thermodynamics. J. Mol. Liq., 298, 112001 (2020).

[10] Gupta V.K., Agarwal S., Sadegh H., Ali G.A.M., Bharti A.K., Hamdy A.S. Facile route synthesis of novel graphene oxide-β-cyclodextrin nanocomposite and its application as adsorbent for removal of toxic bisphenol A from the aqueous phase. J. Mol. Liq., 237, 466–472 (2017).

[11] Agarwal S., Sadegh H., Monajjemi Majid, Makhlouf A.S.H., Ali G.A.M., Memar A.O.H., Shahryari-ghoshekandi R., Tyagi I., Gupta V.K. Efficient removal of toxic bromothymol blue and methylene blue from wastewater by polyvinyl alcohol. J. Mol. Liq., 218, 191-197 (2016).

[12] Shayegan H., Ali G.A.M., Safarifard V. Amide-Functionalized Metal–Organic Framework for High Efficiency and Fast Removal of Pb(II) from Aqueous Solution. Journal of Inorganic and Organometallic Polymers and Materials, 30, 3170–3178 (2020).

[13] Ali G.A.M., Barhoum A., Gupta V.K., Nada A.A., El-Maghrabi H., Kanthasamy R., Shaaban E.R., Algarni H., Chong K.F. High surface area mesoporous silica for hydrogen sulfide effective removal. Current Nanoscience, 16(2), 226-234 (2020).

[14] El-Ghobashy M.A., Khamis M.M., Elsherbiny A.S., Salem I.A. Selective removal of ammonia from wastewater using Cu(II)-loaded Amberlite IR-120 resin and its catalytic application for removal of dyes. Environmental Science and Pollution Research, (2023).

[15] Vajapara S., Pathan A., Bhasin C.P. Adsorption and Photocatalytic Performance of Activated Carbon and Activated Carbon-La_2O_3 nanoparticles Composites for Malachite Green. International Journal of Thin Film Science and Technology, 12(1), 21-37 (2023).

[16] Sanyaolu V.T., Sanyaolu A.A.A., Fadele E. Spatial variation in Heavy Metal residue in Corchorus olitorious cultivated along a Major highway in Ikorodu-Lagos, Nigeria. Journal of Applied Sciences and Environmental Management, 15(2), (2011).

[17] Sharma L., Alam N.M., Roy S., Satya P., Kar G., Ghosh S., Goswami T., Majumdar B. Optimization of alkali pretreatment and enzymatic saccharification of jute (Corchorus olitorius L.) biomass using response surface methodology. Bioresour. Technol., 368, 128318 (2023).

[18] Tovihoudji G.P., Djogbenou C.P., Akponikpe P.B.I., Kpadonou E., Agbangba C.E., Dagbenonbakin D.G. Response of Jute Mallow (Corchorus olitorius L.) to organic manure and inorganic fertilizer on a ferruginous soil in North-eastern Benin. Journal of Applied Biosciences, 92(1), 8610 (2015).

[19] Ndlovu J., Afolayan A.J. Nutritional Analysis of the South African Wild Vegetable Corchorus olitorius L. Asian Journal of Plant Sciences, 7(6), 615-618 (2008).

[20] Abul-Soud M., Mancy A. Urban horticulture of molokhia and spinach environmentally via green roof system and vermicomposting outputs. Global J. Adv. Res, 2(12), 1832-1847 (2015).

[21] Dey S., Basha S.R., Babu G.V., Nagendra T. Characteristic and biosorption capacities of orange peels biosorbents for removal of ammonia and nitrate from contaminated water. Cleaner Materials, 1, 100001 (2021).

[22] Bellahsen N., Varga G., Halyag N., Kertész S., Tombácz E., Hodúr C. Pomegranate peel as a new low-cost adsorbent for ammonium removal. International Journal of Environmental Science and Technology, 18(3), 711-722 (2020).

[23] Ibrahim A., Yusof L., Beddu N.S., Galasin N., Lee P.Y., Lee R.N.S., Zahrim A.Y. Adsorption study of Ammonia Nitrogen by watermelon rind. IOP Conference Series: Earth and Environmental Science, 36, 012020 (2016).

[24] Chakraborty T.K., Islam M.S., Zaman S., Kabir A.H.M.E., Ghosh G.C. Jute (Corchorus olitorius) stick charcoal as a low-cost adsorbent for the removal of methylene blue dye from aqueous solution. SN Applied Sciences, 2(4), 765 (2020).
[25] Rice E.W., Bridgewater L., Association A.P.H., Standard methods for the examination of water and wastewater, American public health association Washington, DC2012.
[26] Fomina E.V., Sverguzova S.V., Sapronova Z.A., Kozhukhova M.I. Obtaining sorption material from sorghum for aqueous solutions purification from heavy metals. IOP Conference Series: Materials Science and Engineering, 945(1), 012016 (2020).
[27] Chen Y., Chen Q., Zhao H., Dang J., Jin R., Zhao W., Li Y. Wheat Straws and Corn Straws as Adsorbents for the Removal of Cr(VI) and Cr(III) from Aqueous Solution: Kinetics, Isotherm, and Mechanism. ACS Omega, 5(11), 6003-6009 (2020).
[28] Molaudzi N.R., Ambushe A.A. Sugarcane Bagasse and Orange Peels as Low-Cost Biosorbents for the Removal of Lead Ions from Contaminated Water Samples. Water, 14(21), 3395 (2022).
[29] Song H.-L., Liang L., Yang K.-Y. Removal of several metal ions from aqueous solution using powdered stem of Arundo donax L. as a new biosorbent. Chem. Eng. Res. Des., 92(10), 1915-1922 (2014).
[30] Tongpoothorn W., Somsimee O., Somboon T., Sriuttha M. An alternative and cost-effective biosorbent derived from napier grass stem for malachite green removal. Journal of Materials and Environmental Sciences, 10(8), 685-695 (2019).
[31] Moubarik A., Grimi N. Valorization of olive stone and sugar cane bagasse by-products as biosorbents for the removal of cadmium from aqueous solution. Food Research International, 73, 169-175 (2015).
[32] Marañón E., Ulmanu M., Fernández Y., Anger I., Castrillón L. Removal of ammonium from aqueous solutions with volcanic tuff. J. Hazard. Mater., 137(3), 1402-1409 (2006).
[33] Emerson K., Russo R.C., Lund R.E., Thurston R.V. Aqueous ammonia equilibrium calculations: effect of pH and temperature. Journal of the Fisheries Board of Canada, 32(12), 2379-2383 (1975).
[34] Anthonisen A.C., The effects of free ammonia and free nitrous acid on the nitrification process, Cornell University1974.
[35] Sulyman M., Namiesnik J., Gierak A. Low-cost Adsorbents Derived from Agricultural By-products/Wastes for Enhancing Contaminant Uptakes from Wastewater: A Review. Polish Journal of Environmental Studies, 26(2), 479-510 (2017).
[36] Ismail Z.Z., Hameed B.B. Recycling of raw corn cob residues as an agricultural waste material for ammonium removal: kinetics, isotherms, and mechanisms. International Journal of Environment and Waste Management, 13(3), 217 (2014).
[37] Sulyman M., Namieśnik J., Gierak A. Utilization of New Activated Carbon Derived from Oak Leaves for Removal of Crystal Violet from Aqueous Solution. Polish Journal of Environmental Studies, 23, (2014).
[38] Abdel Ghafar H.H., Ali G.A.M., Fouad O.A., Makhlouf S.A. Enhancement of adsorption efficiency of methylene blue on Co_3O_4/SiO_2 nanocomposite. Desalination and Water Treatment, 53(11), 2980-2989 (2015).
[39] Preetham V., Vengala J. Removal of agricultural wastewater pollutants by integrating two waste materials, fish scales and neem leaves, as novel potential adsorbent. Water Sci. Technol., 84(10-11), 2980-2996 (2021).
[40] Bhattacharyya K.G., Sharma A. Adsorption of Pb (II) from aqueous solution by Azadirachta indica (Neem) leaf powder. J. Hazard. Mater., 113(1-3), 97-109 (2004).
[41] Elmorsi T.M. Equilibrium isotherms and kinetic studies of removal of methylene blue dye by adsorption onto miswak leaves as a natural adsorbent. Journal of Environmental Protection, 2(06), 817 (2011).
[42] Vijayakumar G., Tamilarasan R., Dharmendirakumar M. Adsorption, Kinetic, Equilibrium and Thermodynamic studies on the removal of basic dye Rhodamine-B from aqueous solution by the use of natural adsorbent perlite. J. Mater. Environ. Sci, 3(1), 157-170 (2012).
[43] Ayawei N., Ebelegi A.N., Wankasi D. Modelling and interpretation of adsorption isotherms. Journal of Chemistry, 2017, (2017).
[44] Temkin M. Kinetics of ammonia synthesis on promoted iron catalysts. Acta Physiochim. URSS, 12, 327-356 (1940).
[45] Dada A., Olalekan A., Olatunya A., Dada O. Langmuir, Freundlich, Temkin and Dubinin–Radushkevich isotherms studies of equilibrium sorption of Zn2+ unto phosphoric acid modified rice husk. IOSR Journal of applied chemistry, 3(1), 38-45 (2012).
[46] Ibrahim M., Sani S. Comparative isotherms studies on adsorptive removal of Congo red from wastewater by watermelon rinds and neem-tree leaves. Open Journal of Physical Chemistry, 4(04), 139 (2014).
[47] Chen H., Zhao J., Dai G., Wu J., Yan H. Adsorption characteristics of Pb (II) from aqueous solution onto a natural biosorbent, fallen Cinnamomum camphora leaves. Desalination, 262(1-3), 174-182 (2010).
[48] Liu H., Dong Y., Liu Y., Wang H. Screening of novel low-cost adsorbents from agricultural residues to remove ammonia nitrogen from aqueous solution. J. Hazard. Mater., 178(1), 1132-1136 (2010).
[49] Bellahsen N., Varga G., Halyag N., Kertész S., Tombácz E., Hodúr C. Pomegranate peel as a new low-cost adsorbent for ammonium removal. International Journal of Environmental Science and Technology, 18(3), 711-722 (2021).
[50] Khalil A., Sergeevich N., Borisova V. Removal of ammonium from fish farms by biochar obtained from rice straw: Isotherm and kinetic studies for ammonium adsorption. Adsorption Science & Technology, 36(5-6), 1294-1309 (2018).
[51] Cheng H., Zhu Q., Xing Z. Adsorption of ammonia nitrogen in low temperature domestic wastewater by modification bentonite. Journal of Cleaner Production, 233, 720-730 (2019).
[52] Sharifnia S., Khadivi M.A., Shojaeimehr T., Shavisi Y. Characterization, isotherm and kinetic studies for ammonium ion adsorption by light expanded clay aggregate (LECA). Journal of Saudi Chemical Society, 20, S342-S351 (2016).
[53] Boopathy R., Karthikeyan S., Mandal A.B., Sekaran G. Adsorption of ammonium ion by coconut shell-

activated carbon from aqueous solution: kinetic, isotherm, and thermodynamic studies. Environmental Science and Pollution Research, 20(1), 533-542 (2013).
[54] Jellali S., Wahab M.A., Anane M., Riahi K., Jedidi N. Biosorption characteristics of ammonium from aqueous solutions onto Posidonia oceanica (L.) fibers. Desalination, 270(1), 40-49 (2011).
[55] Seruga P., Krzywonos M., Pyżanowska J., Urbanowska A., Pawlak-Kruczek H., Niedźwiecki Ł. Removal of Ammonia from the Municipal Waste Treatment Effluents using Natural Minerals. Molecules, 24(20), 3633 (2019).
[56] Vaičiukynienė D., Mikelionienė A., Baltušnikas A., Kantautas A., Radzevičius A. Removal of ammonium ion from aqueous solutions by using unmodified and H2O2-modified zeolitic waste. Scientific Reports, 10(1), 352 (2020).
[57] Puari A.T., Rusnam, Yanti N.R. Removal of Ammonium by Biochar Derived from Exhausted Coffee Husk (ECH) at Different Carbonisation Parameter. IOP Conference Series: Earth and Environmental Science, 1182(1), 012037 (2023).
[58] Martins A.E., Pereira M.S., Jorgetto A.O., Martines M.A., Silva R.I., Saeki M.J., Castro G.R. The reactive surface of Castor leaf [Ricinus communis L.] powder as a green adsorbent for the removal of heavy metals from natural river water. Appl. Surf. Sci., 276, 24-30 (2013).
[59] Qiu H., Lv L., Pan B.-c., Zhang Q.-j., Zhang W.-m., Zhang Q.-x. Critical review in adsorption kinetic models. Journal of Zhejiang University-Science A, 10(5), 716-724 (2009).
[60] Ho Y.-S., McKay G. Pseudo-second order model for sorption processes. Process Biochem., 34(5), 451-465 (1999).
[61] McLintock I. The Elovich equation in chemisorption kinetics. Nature, 216, 1204-1205 (1967).
[62] Lagergren S.K. About the theory of so-called adsorption of soluble substances. Sven. Vetenskapsakad. Handingarl, 24, 1-39 (1898).
[63] Ho Y.S., McKay G. The kinetics of sorption of divalent metal ions onto sphagnum moss peat. Water Res., 34(3), 735-742 (2000).
[64] Cheung C.W., Porter J.F., McKay G. Elovich equation and modified second-order equation for sorption of cadmium ions onto bone char. Journal of Chemical Technology & Biotechnology, 75(11), 963-970 (2000).
[65] Ho Y.S., McKay G. A comparison of chemisorption kinetic models applied to pollutant removal on various sorbents. Process Safety and Environmental Protection, 76(4), 332-340 (1998).
[66] Tseng R.-L., Wu F.-C., Juang R.-S. Liquid-phase adsorption of dyes and phenols using pinewood-based activated carbons. Carbon, 41(3), 487-495 (2003).
[67] Priyantha N., Bandaranayaka A. Investigation of kinetics of Cr (VI)–fired brick clay interaction. J. Hazard. Mater., 188(1-3), 193-197 (2011).
[68] Weber Jr W.J., Morris J.C. Kinetics of adsorption on carbon from solution. Journal of the sanitary engineering division, 89(2), 31-59 (1963).
[69] Kannan N., Sundaram M.M. Kinetics and mechanism of removal of methylene blue by adsorption on various carbons—a comparative study. Dyes and pigments, 51(1), 25-40 (2001).
[70] Sujana M., Mohanty S. Characterization and fluoride uptake studies of nano-scale iron oxide-hydroxide synthesized by microemulsion method. International Journal of Engineering, Science and Technology, 2(8), (2010).
[71] Gouda G.A.H., Ali G.A.M., Seaf Elnasr T.A. Stability studies of selected metal Ions chelates with 2-(4-amino-1,5-dimethyl-2-phenyl-1,2-dihydro-pyrazol-3-ylideneamino) phenol. International Journal of Nanomaterials and Chemistry, 1(2), 39-44 (2015).
[72] Lima E.C., Hosseini-Bandegharaei A., Moreno-Piraján J.C., Anastopoulos I. A critical review of the estimation of the thermodynamic parameters on adsorption equilibria. Wrong use of equilibrium constant in the Van't Hoof equation for calculation of thermodynamic parameters of adsorption. J. Mol. Liq., 273, 425-434 (2019).
[73] Xu H., Wang B., Zhao R., Wang X., Pan C., Jiang Y., Zhang X., Ge B. Adsorption behavior and performance of ammonium onto sorghum straw biochar from water. Scientific Reports, 12(1), 5358 (2022).
[74] Kennedy L.J., Vijaya J.J., Sekaran G., Kayalvizhi K. Equilibrium, kinetic and thermodynamic studies on the adsorption of m-cresol onto micro-and mesoporous carbon. J. Hazard. Mater., 149(1), 134-143 (2007).